Thermal Gradient Cyclic Behavior of a Thermal/Environmental Barrier Coating System on SiC/SiC Ceramic Matrix Composites

Dongming Zhu
Ohio Aerospace Institute, Brook Park, Ohio

Kang N. Lee
Cleveland State University, Cleveland, Ohio

Robert A. Miller
Glenn Research Center, Cleveland, Ohio

The NASA STI Program Office . . . in Profile

Since its founding, NASA has been dedicated to the advancement of aeronautics and space science. The NASA Scientific and Technical Information (STI) Program Office plays a key part in helping NASA maintain this important role.

The NASA STI Program Office is operated by Langley Research Center, the Lead Center for NASA's scientific and technical information. The NASA STI Program Office provides access to the NASA STI Database, the largest collection of aeronautical and space science STI in the world. The Program Office is also NASA's institutional mechanism for disseminating the results of its research and development activities. These results are published by NASA in the NASA STI Report Series, which includes the following report types:
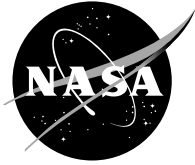
- TECHNICAL PUBLICATION. Reports of completed research or a major significant phase of research that present the results of NASA programs and include extensive data or theoretical analysis. Includes compilations of significant scientific and technical data and information deemed to be of continuing reference value. NASA's counterpart of peer-reviewed formal professional papers but has less stringent limitations on manuscript length and extent of graphic presentations.

- TECHNICAL MEMORANDUM. Scientific and technical findings that are preliminary or of specialized interest, e.g., quick release reports, working papers, and bibliographies that contain minimal annotation. Does not contain extensive analysis.

- CONTRACTOR REPORT. Scientific and technical findings by NASA-sponsored contractors and grantees.

- CONFERENCE PUBLICATION. Collected papers from scientific and technical conferences, symposia, seminars, or other meetings sponsored or cosponsored by NASA.

- SPECIAL PUBLICATION. Scientific, technical, or historical information from NASA programs, projects, and missions, often concerned with subjects having substantial public interest.

- TECHNICAL TRANSLATION. English-language translations of foreign scientific and technical material pertinent to NASA's mission.

Specialized services that complement the STI Program Office's diverse offerings include creating custom thesauri, building customized data bases, organizing and publishing research results . . . even providing videos.

For more information about the NASA STI Program Office, see the following:

- Access the NASA STI Program Home Page at *http://www.sti.nasa.gov*

- E-mail your question via the Internet to help@sti.nasa.gov

- Fax your question to the NASA Access Help Desk at 301–621–0134

- Telephone the NASA Access Help Desk at 301–621–0390

- Write to:
  NASA Access Help Desk
  NASA Center for AeroSpace Information
  7121 Standard Drive
  Hanover, MD 21076

Thermal Gradient Cyclic Behavior of a Thermal/Environmental Barrier Coating System on SiC/SiC Ceramic Matrix Composites

Dongming Zhu
Ohio Aerospace Institute, Brook Park, Ohio

Kang N. Lee
Cleveland State University, Cleveland, Ohio

Robert A. Miller
Glenn Research Center, Cleveland, Ohio

National Aeronautics and
Space Administration

Glenn Research Center

May 2002

Acknowledgments

GT–2002–30632

THERMAL GRADIENT CYCLIC BEHAVIOR OF A THERMAL/ENVIRONMENTAL BARRIER COATING SYSTEM ON SIC/SIC CERAMIC MATRIX COMPOSITES

Dongming Zhu
Ohio Aerospace Institute
Brook Park, Ohio 44135

Kang N. Lee
Cleveland State University
Cleveland, Ohio 44115

Robert A. Miller
National Aeronautics and Space Administration
Glenn Research Center
Cleveland, Ohio 44135

ABSTRACT

Thermal barrier and environmental barrier coatings (TBCs and EBCs) will play a crucial role in future advanced gas turbine engines because of their ability to significantly extend the temperature capability of the ceramic matrix composite (CMC) engine components in harsh combustion environments. In order to develop high performance, robust coating systems for effective thermal and environmental protections of the engine components, appropriate test approaches for evaluating the critical coating properties must be established. In this paper, a laser high-heat-flux, thermal gradient approach for testing the coatings will be described. Thermal cyclic behavior of plasma-sprayed coating systems, consisting of ZrO_2-8wt%Y_2O_3 thermal barrier and NASA Enabling Propulsion Materials (EPM) Program developed mullite+BSAS/Si type environmental barrier coatings on SiC/SiC ceramic matrix composites, was investigated under thermal gradients using the laser heat-flux rig in conjunction with the furnace thermal cyclic tests in water-vapor environments. The coating sintering and interface damage were assessed by monitoring the real-time thermal conductivity changes during the laser heat-flux tests and by examining the microstructural changes after the tests. The coating failure mechanisms are discussed based on the cyclic test results and are correlated to the sintering, creep, and thermal stress behavior under simulated engine temperature and heat flux conditions.

INTRODUCTION

Environmental barrier coatings (EBCs) have been developed to protect SiC-based ceramic components in gas turbine engines from high temperature environmental attack [1–5]. With continuously increasing demands for significantly higher engine operating temperature, future EBC systems must be designed for both thermal and environmental protection of the engine components in gas turbine combustion environments [6]. In particular, thermal barrier functions of EBCs become necessary for reducing the engine component thermal loads and chemical reaction rates, while still maintaining required mechanical properties and durability of these components. The advances in thermal and environmental barrier coating (TBC and EBC) development will directly impact the successful use of ceramic components in advanced engines.

In order to develop high performance ceramic coating systems, advanced high-heat-flux test approaches need to be established. The high-heat-flux test rigs will not only be able to heat the coating surface to significantly higher temperatures (e.g., 1500°C to 1650°C), but will also establish a large thermal gradient across the coating thickness. In this way, the coating/substrate interface and the substrate can be maintained below a safe temperature limit. The coating operating temperature and stress conditions can also be more realistically simulated during such a test.

The laser high-heat-flux test rigs were developed for durability testing of thermal barrier coatings [7–13]. The coating thermal conductivity and sintering properties can be measured in real-time from this kind of test. In addition, coating delaminations can be monitored as a function of cycles from the observed thermal conductivity variations because coating delamination cracking causes a decrease in the measured

thermal conductivity. The laser approach has also been demonstrated in evaluating environmental barrier coatings on SiC/SiC substrates [14].

In this study, the laser high-heat-flux based technique has been employed to investigate thermal cyclic behavior of a multi-layered ZrO_2-8wt%Y_2O_3, and EPM bond coat type mullite + barium-strontium-aluminosilicate (BSAS) mixture/Si TBC/EBC system on SiC/SiC ceramic matrix composite substrates. In some cases, the laser thermal gradient tests in ambient air were combined with furnace thermal cyclic tests in water-vapor environments for testing the coating specimens, providing information about the water-vapor effects on coating failure. The coating thermal conductivity, sintering, cracking and delamination were evaluated during the thermal cycling tests. Coating failure mechanisms are discussed based on the cyclic test results and are correlated with the sintering, creep, and thermal stress behavior as a function of the test temperature and heat flux conditions.

EXPERIMENTAL
Plasma-sprayed ZrO_2-8wt%Y_2O_3 thermal and mullite+BSAS/Si environmental barrier coatings on SiC/SiC ceramic matrix composites were investigated in this study. The EBC systems, namely, mullite and BSAS mixture layer and Si bond coat, were air plasma-sprayed (APS) onto the 25.4 mm-diameter and ~2.1 mm-thick melt infiltrated (MI) SiC/SiC ceramic composites substrates on a hot stage of a furnace in order to ensure crystalline phases of these coating materials. The top ZrO_2-8wt%Y_2O_3 coating was then deposited using a conventional APS technique. The nominal thicknesses of the coating system are listed in Table 1.

Table 1. TBC/EBC coating system investigated in this study

	Top TBC	EBC system		Substrate
Coating Materials	ZrO_2-8wt%Y_2O_3 (µm)	Mullite +BSAS (µm)	Si (µm)	MI SiC$_f$/SiC (mm)
Thick-nesses	210-290	290-370	90-170	1.9-2.3

Thermal gradient cyclic testing of the ceramic coating materials was carried out using a 3.0 kW CO_2 laser (wavelength 10.6 micron) high-heat-flux rig. The general test approaches have been described elsewhere [10, 14-16]. In this laser heat flux test, coating surface heating was provided by the laser beam and backside air cooling was used to maintain the desired specimen temperatures. A uniform laser heat flux was obtained over the 23.9 mm diameter aperture region of the specimen surface by using an integrating ZnSe lens combined with specimen rotation. Platinum wire flat coils (wire diameter 0.38 mm) were used to form thin air gaps between the top platinum-coated stainless-steel plate and bottom stainless-steel back plate to minimize specimen heat loss through the fixture. During the laser thermal cycling test, the coating surface temperature was measured by an 8 µm infrared pyrometer and the backside CMC surface was measured by a two-color pyrometer. The real-time thermal conductivity of the coating system can also be obtained by measuring the temperature difference across the coating system.

The TBC/EBC coatings were thermal cycled in ambient air under the laser imposed thermal gradients. The surface was tested at approximately 1482°C, and the coating/substrate interface temperature was at 1250°C or 1300°C. Thermal conductivity of the ceramic coating system was also monitored as a function of the laser cycle number using the steady-state laser heat flux test approach [10, 14–17]. Some coating specimens were also subjected to alternating laser thermal gradient cycling tests in air and furnace thermal cycling tests in a 90%H_2O-balance O_2 water vapor environment at 1300°C. The laser thermal cyclic tests were conducted using either 30 or 60 min hot time temperature cycles, but all with 3 min cooling between each cycle to ensure that the test specimens were cooled below 100°C. Furnace cyclic tests consisted of 60 min high temperature heating and 20 min cooling cycles.

RESULTS
Thermal Conductivity
Fig. 1 shows the thermal conductivity of a 0.58 mm thick ZrO_2-8wt%Y_2O_3/mullite+BSAS coating system during a 20 hr steady-state test under the laser high-heat-flux conditions. The coating had an initial conductivity about 1.7 W/m-K. After laser thermal exposure at 1482°C surface temperature and 1250°C coating/substrate interface temperature, the average coating conductivity value increased to 2.35 W/m-K in about 3 hours. The conductivity then decreased with the test time. At the end of the 20 hours, the coating conductivity was about 1.9 W/m-K.

This coating specimen was further subjected to a combined test consisting of both furnace thermal cycling in a 90% water vapor environment and laser thermal gradient cycling in air. The coating thermal conductivity was measured in-situ during the laser portion of the thermal cyclic test, and the results are shown in Fig. 2. It can be seen that the alternating furnace and laser thermal cyclic tests resulted in significant coating thermal conductivity variations (i.e. large conductivity increases or decreases). The coating conductivity changed from the highest value 2.3 W/m-K during the first laser test cycle to about 1.5 W/m-K after the 400 combined laser and furnace cyclic tests.
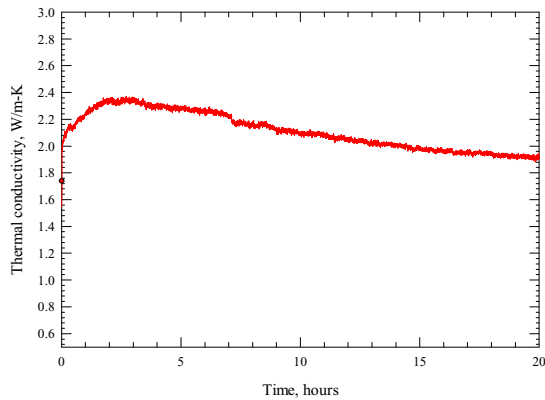
Fig. 1 Thermal conductivity of a 0.58 mm thick ZrO_2-8wt%Y_2O_3/mullite+BSAS coating system during 20 hr laser steady-state testing. The coating surface and interface test temperatures were 1482°C and 1250°C, respectively.
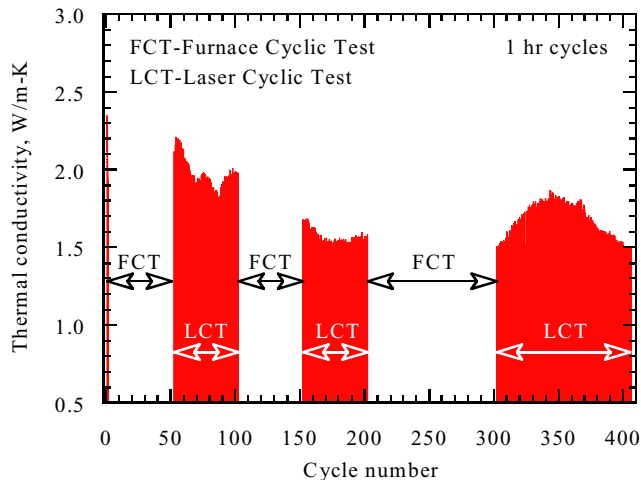

Fig. 2 Thermal conductivity variations of a 0.58 mm thick ZrO_2-8wt%Y_2O_3/mullite+BSAS coating system during the combined laser thermal gradient cyclic test in air (with the coating surface and interface test temperatures at 1482°C and 1250°C) and the furnace thermal cyclic test in 90% water vapor environment at 1300°C. The 60 min hot time cycles were used for both the laser and furnace tests.

After exposure for the first 50 furnace cycles, the coating thermal conductivity increased from 1.9 W/m-K (measured after the first 20 hr laser testing) to 2.1 W/m-K. During subsequent 50 laser test cycles, the coating conductivity first increased to about 2.2 W/m-K, and then generally decreased as the cycles increased, dropping down to about 2.0 W/m-K at the end of the laser test cycles. During the rest of the furnace and

laser thermal cycles, the overall coating conductivity showed a general trend to decrease with further thermal cycling. The largest conductivity reduction (~17% reduction) was observed after the second 50 furnace cycles. The thermal conductivity changes after each segment of laser or furnace cycling are illustrated in Table 2.

Table 2. Thermal conductivity (k) changes during the combined laser cyclic test (LCT) and furnace cyclic test (FCT)

Cycle type (test time)	Laser Steady-state	FCT	LCT	FCT	LCT	FCT	LCT
	(20hr test)	(1 hr cycles)					
Test cycles	1	2-51	52-101	102-151	152-201	202-301	302-401
k %change	+12	+10	-6	-17	-4.2	-4.4	-2

Fig. 3 shows the measured thermal conductivity of a 0.58 mm thick ZrO_2-8wt%Y_2O_3/mullite+BSAS coating system as a function of cycles using only the laser thermal gradient cyclic test. The laser test conditions for this specimen were the same as that for the specimen which was tested with the combined laser and furnace tests, i.e., surface and interface temperatures of 1482°C and 1250°C, respectively, and with 1 hr hot time cycles. The test results showed that the average coating conductivity for this specimen also increased to about 2.3 W/m-K during first several cycles. However, the specimen exposed only to the laser cycling exhibited a monotonic decrease in coating conductivity after the conductivity reached a peak value of 2.3 W/m-K. The coating thermal conductivity remained relatively unchanged after 40 hr laser testing. The coating conductivity had a higher value of 1.8 W/m-K after the 134 cycles of the laser thermal gradient cyclic testing, as compared to the previous laser and furnace tested specimen that had a conductivity of 1.6-1.7 W/m-K after the same number of test cycles.

Fig. 4 shows the thermal conductivity of a 0.58 mm thick ZrO_2-8wt%Y_2O_3/mullite+BSAS coating systems as a function of cycles using only the laser thermal gradient cyclic test at a higher interface test temperature of about 1300°C and a 30 min shorter hot cycle time. The surface test temperature was still maintained at about 1482°C. Note in Fig. 4 that more conductivity variations were observed in this test than in the laser testing conducted at a lower interface temperature. It can be seen that the coating reached a peak conductivity value of

about 2.25 W/m-K after about 5 cycles, decreased to about 1.85 W/m-K after 25 cycles, then increased again to about 2.1 W/m-K after 70 laser cycles. Further testing resulted in a conductivity reduction, reaching about 1.65 W/m-K after 200 laser cycles. A similar conductivity reduction (from 2.3 W/m-K to 1.6 W/m-K) was observed for the combined laser and furnace cyclic test after total 200 cycles, but it took twice as long because 60 min cycling was used for the laser and furnace combined cycle tests. The accelerated conductivity reduction (the same amount of conductivity reduction in less time) was observed for the more frequent cycle test (30 min cycle test) as compared to the 60 min cycle tests.
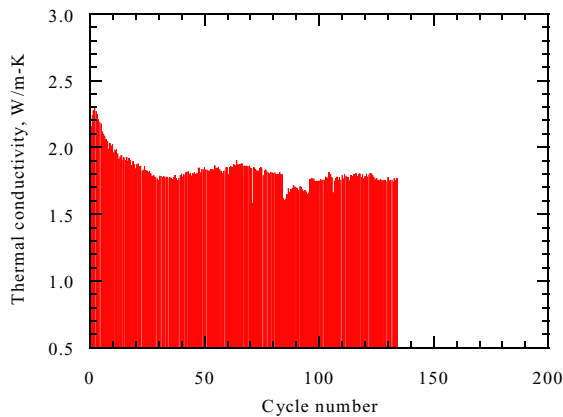

Fig. 3 Thermal conductivity variations of a 0.58 mm thick ZrO_2-8wt%Y_2O_3/mullite+BSAS coating system during the 60 min hot time cycle laser thermal gradient test, with the coating surface and interface test temperatures being at 1482°C and 1250°C, respectively.
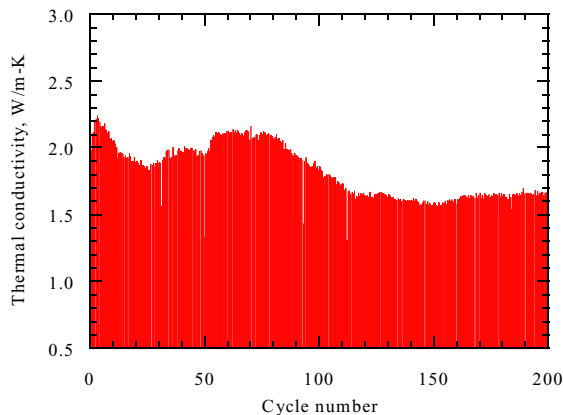

Fig. 4 Thermal conductivity variations of a 0.58 mm thick ZrO_2-8wt%Y_2O_3/mullite+BSAS coating system during the 30 min hot time cycle laser thermal gradient test, with the coating surface and interface test temperatures being at 1482°C and 1300°C, respectively.

Failure Modes

The coating failure modes were investigated during the laser and combined laser/furnace cyclic tests. Fig. 5 shows typical coating surface and cross-section cracking morphologies after the laser high thermal gradient tests. As shown in Fig. 5 (a), extensive "mud-flat" cracking was developed on the coating surface after 134 cycles laser testing (60 min hot time laser cycling). The size of the major surface crack segments typically ranged from 0.5 to 1 mm. This typical surface cracking pattern was observed for all the tested specimens. Surface cracking was found to occur even at early stages of the laser testing (e.g., after the 20 hr laser steady-state cycle test), although the crack widths and crack density usually increased with test cycles. From the cross-section micrographs of the tested coating specimen shown in Fig. 5 (b), it can be seen that the surface cracks tended to be wedge-shaped, with the larger crack opening widths near the coating surface and within the ZrO_2-8wt%Y_2O_3 layer. The cracks that initiated from the coating surface extended deeply into the mullite and BSAS mixture layers under the thermal cyclic loading, resulting in severe EBC coating damage and the subsequent overall TBC/EBC coating delamination.

The spallation morphologies of the 25.4 mm diameter coating specimens were captured using a fast-speed video camera during the laser testing, as shown in Fig. 6. Because the delaminated coatings will show a higher brightness contrast due to higher surface temperatures under the laser heating conditions, the bright regions in the captured images represented the delaminated and spalled coatings. Fig. 6 (a) shows the coating failure image after 400 cycles of the combined laser and furnace cyclic tests (60 min hot time cycles, laser test surface and interface temperatures at 1482°C and 1250°C, respectively, and furnace test temperature at 1300°C). It can be seen that besides coating spallations in the middle region of the specimen, extensive coating delaminations and spallations also occurred near the specimen edges because the exposure of the entire specimen during the furnace thermal cycles resulted in severe edge stress concentration and thus edge crack initiation. Fig. 6 (b) shows the coating spallation image of the laser cyclic tested specimen without furnace exposure (30 min hot cycles, laser test surface temperature 1482°C and interface temperature of 1300°C). For this specimen, the edge cracking was suppressed because the laser aperture top plate effectively shielded the coating edges and thus more or less prevented the coating edge failure. The coating had large spalled areas primarily near the center of the specimen.

It should be noted that the coating failure observed under the present testing was still at the relatively early stages where

some large isolated coating pieces about several millimeters (up to 9-10 mm) in size were delaminated and later spalled off. The laser testing was interrupted to avoid further catastrophic spallation and possible melting of the coatings due to laser heating (as has been observed in some of early tests) in order to preserve better evidence for investigating coating failure mechanisms.

DISCUSSION

For both the laser and combined laser/furnace tested specimens, initial thermal conductivity increased considerably due to coating sintering. Increased thermal conductivity for ZrO_2-8wt%Y_2O_3 thermal barrier and Si-based environmental barrier coatings has been experimentally demonstrated [10, 14–16]. The modeled thermal conductivity increases for a ZrO_2-8wt% Y_2O_3 coating as a function of time and temperature using the previous test data are shown in Fig. 7. It should be pointed out that the data were measured for the ZrO_2-8wt% Y_2O_3 coating material at a lower temperature regime (1000–1300°C), and the extrapolation to higher temperatures may be considered qualitative and should be used with great caution. Nevertheless, the results show that a very fast conductivity increase is expected for ZrO_2-8wt%Y_2O_3 coating system at all the test temperatures.

For BSAS and mullite/BSAS environmental barrier coatings, it has been reported that the combined laser cyclic test in air and furnace cyclic test in water vapor caused faster coating sintering and more conductivity increases at the initial cyclic stage than the laser thermal cycling test in air [14]. In the present study, the combined laser and furnace tests resulted in higher overall conductivity increases in the first 100-120 cycles for the TBC/EBC system as compared to the laser tests in air, which is consistent with the previous observations. The enhanced coating sintering under the combined laser and furnace cycle tests may be attributed to the enhanced sintering of the ceramic coatings at the higher test interface temperature and the enhanced EBC sintering due to faster silica formation in the water vapor environments during the furnace cyclic test [17].

The coating conductivity decreases observed under cyclic testing are primarily due to coating cracking and delaminations. The processes are complex in nature and are related to the coating sintering-creep (a time- and temperature-dependent process) and cyclic fatigue (a cycle frequency dependent process) under thermal cycling conditions. It should be mentioned that the conductivity decrease was observed in the first 20 hr steady-state laser testing, indicating possible crack formation and coating delamination due to the large sintering shrinkage at high temperature before the first cooling cycle. After the laser cyclic testing, extensive surface cracks
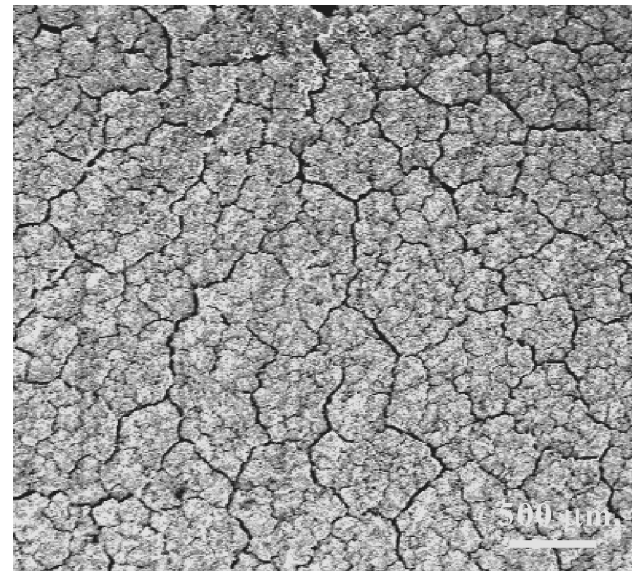

(a)
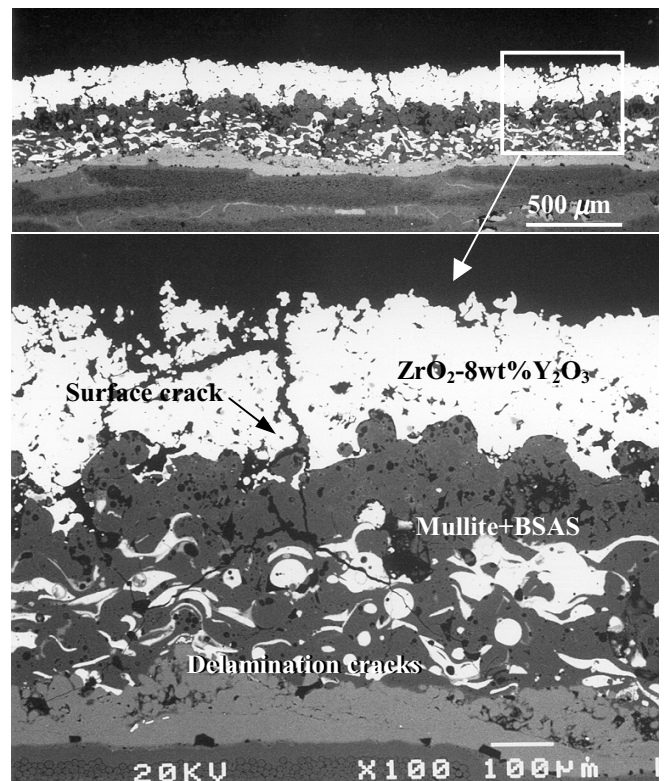
(b)

Fig. 5 Micrographs of typical coating surface and cross-section cracking morphologies of a ZrO_2-8wt%Y_2O_3/mullite+BSAS/Si multi-layered coating system after laser thermal gradient cyclic testing. (a) Coating surface morphology showing extensive surface crack networks developed after laser testing; (b) Coating cross-sections showing the sintered coating layers, and wedge-shape surface cracks and the resulting coating delaminations under the laser thermal gradient cyclic test conditions.
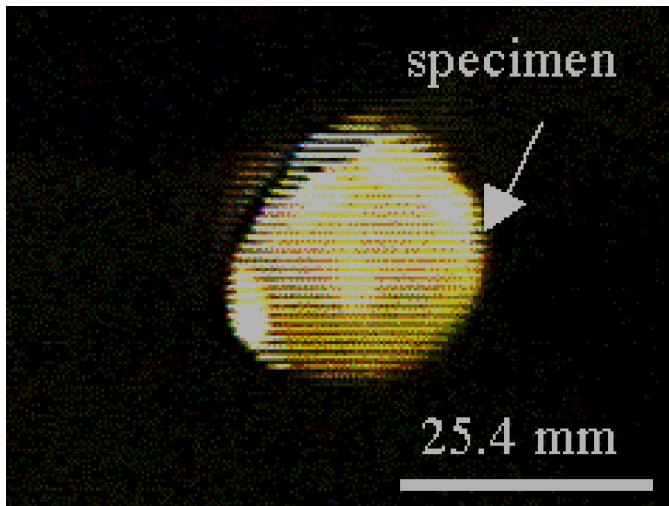
(a)
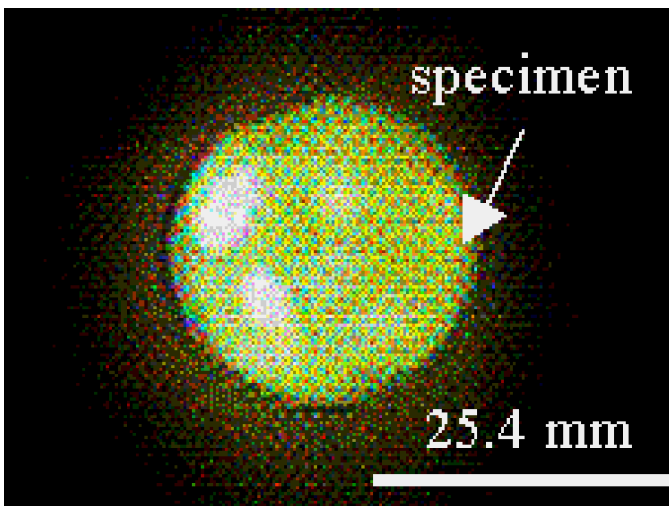
(b)

Fig. 6 Coating spallation images captured for 25.4 mm diameter coating specimens using a fast-speed video camera during the laser testing. Coating delamination and resulting spallation patterns for (a) the combined laser and furnace tested specimen after 400 cycles testing (the 60 min hot cycle) and (b) laser cyclic tested specimen after 200 cycles at the surface and interface temperatures 1482°C and 1300°C, respectively (30 min hot cycles).

developed. The wedge–shaped cracks are often generated due not only to the ceramic coating sintering and creep at high temperature under the laser testing [8], but also to the thermal expansion mismatches between the coating layers and the substrate [17]. Thus, one can correlate the cracking morphologies to the laser thermal gradients and cyclic conditions, and predict the surface crack evolution as a function of time [8].
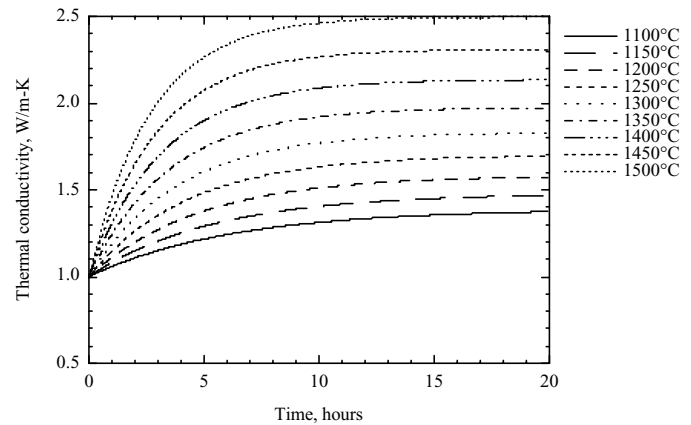

Fig. 7 Thermal conductivity increases as a function of time and temperature predicted and extrapolated from laser tested data for a plasma-sprayed ZrO_2-8wt%Y_2O_3 coating.

The sintering part of the shrinkage for ZrO_2-8wt%Y_2O_3 in the absence of a compressive stress creep was demonstrated in a dilatometer test [17]. The results are shown in Fig. 8. It can be seen that the coating shrinkage strain was about 1.05% after 76 hr isothermal testing at 1500°C. The very fast initial increase in the sintering shrinkage strain will result in the formation of the surface cracks in relatively short test times. Once the surface cracks are formed, the coating delamination cracks will then be initiated and propagated under the cyclic thermal stresses originating from further sintering-creep shrinkages, and the thermal expansion mismatch between the ZrO_2-8wt%Y_2O_3 top-coat, and the Si-based EBCs and CMC substrate during the testing [17]. The conductivity variations during the laser tests are attributed to a competing process of the sintering related crack healing, and new crack formation and crack propagation under thermal cycling conditions.

More severe coating delaminations, as indicated by lower apparent coating conductivities, were observed for the specimen under the combined furnace water vapor and laser cyclic test conditions and for the specimen tested under a higher interface temperature with shorter cycle times. It was previously reported that water vapor had a detrimental effect on EBC coating durability by promoting coating/substrate interfacial pore formation for the current EBC systems under the combined laser thermal gradient (tested at surface and interface temperatures of 1482°C and 1300°C) and furnace water vapor (tested at 1300°C) cyclic testing conditions [14], which leads to faster coating conductivity reductions under the laser thermal cyclic testing. The surface vertical cracks penetrating through the TBC/EBC system will further accelerate coating degradation. When large enough sized pores or cracks are generated under the thermal cycling tests, the crack healing

process will become less favorable or even impossible at the test temperatures. The higher interface test temperature, which may enhance the initial coating sintering and crack healing, will later result in more coating interface damage and weak interface bonding. As a result of this, substantial coating delamination and spallations were observed for the specimen tested under the combined laser cycling in air and furnace cycling in water vapor environments. Similarly, for the short cycle time tested specimens, the crack healing process is also less favorable because of the shorter hold time; more accumulated coating damage due to the more frequent cycles and the weakened interface from the higher interface temperature led to an accelerated coating delamination as observed in the experiments. The accelerated damage with increasing cycle frequency under more frequent cycle test (30 min cycle test) also suggests a possible cyclic fatigue effect besides the time dependent sintering-creep effect for the TBC/EBC coating systems.
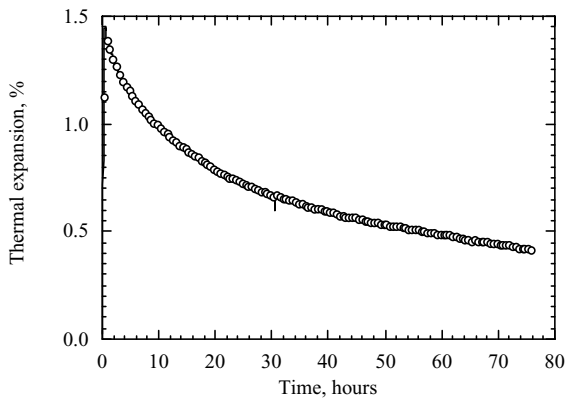

Fig. 8 The sintering-shrinkage strain measured for a plasma-sprayed ZrO_2-8wt%Y_2O_3 coating in a dilatometer thermal expansion test as a function of test time at 1500°C.

CONCLUSIONS

A laser heat flux test approach has been developed to investigate the thermal conductivity and cyclic behavior of plasma-sprayed ZrO_2-8wt%Y_2O_3 thermal barrier and BSAS+mullite/Si environment barrier layered coatings on SiC/SiC ceramic matrix composites under thermal gradient cyclic conditions. The furnace water vapor cyclic tests were also incorporated into the laser cyclic tests to investigate the combined effect of water vapor exposure and thermal gradient cycling on coating conductivity and failure. For both the laser and combined laser-furnace tested specimens, thermal conductivity initially increased due to the coating sintering. The

coating conductivity later decreased under the further cyclic testing due to the coating cracking, delamination and spallation. The failure of the coating system can be characterized as wedge-shaped surface coating cracking, surface cracking-enhanced coating delamination and interface debonding and spallation under the thermal cyclic loading. Enhanced coating sintering and coating delaminations were observed for the specimen under the combined laser cyclic and furnace water vapor test conditions. The accelerated coating delamination with increasing interface test temperature and cycle frequency was also observed for the TBC/EBC coating system.

REFERENCES

[1] K.N. Lee and R.A. Miller, "Development and Environmental Durability of Mullite and Mullite/YSZ Dual Layer Coatings for SiC and Si_3N_4 Ceramics," *Surface and Coatings Technology*, vol. 86–87, pp. 142–148, 1996.

[2] K.N. Lee, "Key Durability Issues with Mullite-Based Environmental Barrier Coatings for Si-Base Ceramics," *Transactions of the ASME*, vol. 122, pp. 632–636, 2000.

[3] K.N. Lee, "Current Status of Environmental Barrier Coatings for Si-Based Ceramics," *Surface and Coatings Technology*, vol. 133–134, pp. 1–7, 2000.

[4] H.E. Eaton, G.D. Linsey, K.L. More, J.B. Kimmel, J.R. Price, and N. Miriyala, "EBC Protection of SiC/SiC Composites in Gas Turbine Combustion Environments," ASME Paper 2000–GT–0631, presented at The International Gas Turbine and Aeroengine Congress and Exposition, Munich, Germany, May 8–11, 2000.

[5] K.L. More, P.F. Tortorelli, L.R. Walker, K.S. Trent, H.E. Eaton, E.Y. Sun, G.D. Linsey, N. Miriyala, J.B. Kimmel, J.R. Price, W.A. Ellingson, J.G. Sun, D.J. Landini, and P. Craig, "Recent Evaluation of CFCC Combustor Liners with Environmental Barrier Coatings (EBCs) after a ~14,000h Engine Test," presented at The International Gas Turbine and Aeroengine Congress and Exposition, New Orleans, LA, USA, June 5–9, 2001.

[6] D. Zhu, K.N. Lee, and R.A. Miller, "Thermal Conductivity and Thermal Gradient Cyclic Behavior of Refractory Silicate Coatings on SiC/SiC Ceramic Matrix Composites," NASA Glenn Research Center, Cleveland, Ohio, NASA TM–210824, April 2001.

[7] D. Zhu and R.A. Miller, "Investigation of Thermal High Cycle and Low Cycle Fatigue Mechanisms of Thick Thermal Barrier Coatings," *Materials Science and Engineering*, vol. A245, pp. 212–223, 1998.

[8] D. Zhu and R.A. Miller, "Determination of Creep Behavior of Thermal Barrier Coatings under Laser Imposed High Thermal and Stress Gradient Conditions," *Journal of Materials Research*, vol. 14, pp. 146–161, 1999.

[9] D. Zhu and R.A. Miller, "Thermophysical and Thermomechanical Properties of Thermal Barrier Coating Systems," *Ceram. Eng. Sci. Proc.*, vol. 21, pp. 623–633, 2000.

[10] D. Zhu and R.A. Miller, "Thermal Barrier Coatings for Advanced Gas-Turbine Engines," *MRS Bulletin*, vol. 27, pp. 43–47, 2000.

[11] D. Zhu and R.A. Miller, "Thermophysical and Thermomechanical Properties of Thermal Barrier Coating Systems," NASA Glenn Research Center, Cleveland, Ohio, NASA TM–210237, July 2000.

[12] D. Zhu, R.A. Miller, B.A. Nagaraj, and R.W. Bruce, "Thermal Conductivity of EB-PVD Thermal Barrier Coatings Evaluated by a Steady-State Laser Heat Flux Technique," *Surface and Coatings Technology*, vol. 138, pp. 1–8, 2001.

[13] D. Zhu, S.R. Choi, and R.A. Miller, "Thermal Fatigue and Fracture Behavior of Ceramic Thermal Barrier Coatings," *Ceram. Eng. and Sci. Proc.*, vol. 22, pp. 453–461, 2001.

[14] D. Zhu, K.N. Lee, and R.A. Miller, "Thermal Conductivity and Thermal Gradient Cyclic Behavior of Refractory Silicate Coatings on SiC/SiC Ceramic Matrix Composites," *Ceram. Eng. Sci. Proc.*, vol. 22, pp. 443–452, 2001.

[15] D. Zhu and R.A. Miller, "Thermal Conductivity and Elastic Modulus Evolution of Thermal Barrier Coatings Under High Heat Flux Conditions," *Journal of Thermal Spray Technology*, vol. 9, pp. 175–180, 2000.

[16] D. Zhu, N.P. Bansal, K.N. Lee, and R.A. Miller, "Thermal Conductivity of Ceramic Thermal Barrier and Environmental Barrier Coating Materials," NASA Glenn Research Center, Cleveland, Ohio, NASA TM–211122, September 2001.

[17] D. Zhu, K.N. Lee, and R.A. Miller, "Sintering and Cyclic Failure Mechanisms of Multi-Layered Thermal and Environmental Barrier Coating Systems under High Thermal Gradient Test Conditions," *Ceram. Eng. Sci. Proc.*, vol. 23, in press.

REPORT DOCUMENTATION PAGE

1. AGENCY USE ONLY (Leave blank)	2. REPORT DATE	3. REPORT TYPE AND DATES COVERED
	May 2002	Technical Memorandum

4. TITLE AND SUBTITLE

Thermal Gradient Cyclic Behavior of a Thermal/Environmental Barrier Coating System on SiC/SiC Ceramic Matrix Composites

5. FUNDING NUMBERS

WU–714–04–30–00

6. AUTHOR(S)

Dongming Zhu, Kang N. Lee, and Robert A. Miller

7. PERFORMING ORGANIZATION NAME(S) AND ADDRESS(ES)

National Aeronautics and Space Administration
John H. Glenn Research Center at Lewis Field
Cleveland, Ohio 44135–3191

8. PERFORMING ORGANIZATION REPORT NUMBER

E–13377

9. SPONSORING/MONITORING AGENCY NAME(S) AND ADDRESS(ES)

National Aeronautics and Space Administration
Washington, DC 20546–0001

10. SPONSORING/MONITORING AGENCY REPORT NUMBER

NASA TM—2002-211593
GT–2002–30632

11. SUPPLEMENTARY NOTES

Prepared for the Turbo Expo 2002 cosponsored by the American Society of Mechanical Engineers and the International Gas Turbine Institute, Amsterdam, The Netherlands, June 3–6, 2002. Dongming Zhu, Ohio Aerospace Institute, 22800 Cedar Point Road, Brook Park, Ohio 44142; Kang N. Lee, Cleveland State University, Cleveland, Ohio; and Robert A. Miller, NASA Glenn Research Center. Responsible person, Dongming Zhu, organization code 5160, 216–433–5422.

12a. DISTRIBUTION/AVAILABILITY STATEMENT

Unclassified - Unlimited
Subject Categories: 24 and 27   Distribution: Nonstandard

Available electronically at http://gltrs.grc.nasa.gov/GLTRS

This publication is available from the NASA Center for AeroSpace Information, 301–621–0390.

12b. DISTRIBUTION CODE

13. ABSTRACT (Maximum 200 words)

Thermal barrier and environmental barrier coatings (TBCs and EBCs) will play a crucial role in future advanced gas turbine engines because of their ability to significantly extend the temperature capability of the ceramic matrix composite (CMC) engine components in harsh combustion environments. In order to develop high performance, robust coating systems for effective thermal and environmental protections of the engine components, appropriate test approaches for evaluating the critical coating properties must be established. In this paper, a laser high-heat-flux, thermal gradient approach for testing the coatings will be described. Thermal cyclic behavior of plasma-sprayed coating systems, consisting of ZrO_2-8wt%Y_2O_3 thermal barrier and NASA Enabling Propulsion Materials (EPM) Program developed mullite+BSAS/Si type environmental barrier coatings on SiC/SiC ceramic matrix composites, was investigated under thermal gradients using the laser heat-flux rig in conjunction with the furnace thermal cyclic tests in water-vapor environments. The coating sintering and interface damage were assessed by monitoring the real-time thermal conductivity changes during the laser heat-flux tests and by examining the microstructural changes after the tests. The coating failure mechanisms are discussed based on the cyclic test results and are correlated to the sintering, creep, and thermal stress behavior under simulated engine temperature and heat flux conditions.

14. SUBJECT TERMS

Thermal barrier coatings; Environmental barrier coating; Thermal gradient cyclic testing; Si-based ceramic matrix composites

15. NUMBER OF PAGES

14

16. PRICE CODE

17. SECURITY CLASSIFICATION OF REPORT	18. SECURITY CLASSIFICATION OF THIS PAGE	19. SECURITY CLASSIFICATION OF ABSTRACT	20. LIMITATION OF ABSTRACT
Unclassified	Unclassified	Unclassified	